

Quantitative study of the violation of k_{\perp} -factorization in hadroproduction of quarks at collider energies

Hirotsugu Fujii^a, François Gelis^b and Raju Venugopalan^{c,d}

*a Institute of Physics, University of Tokyo,
Komaba, Tokyo 153-8902, Japan.*

b CEA/DSM/SPhT, 91191 Gif-sur-Yvette cedex, France.

*c Physics Department, Brookhaven National Laboratory,
Upton, N.Y. 11973, U.S.A.*

d ECT, Villa Tambosi, Strada delle Tabarelle 286,
I-38050, Villazzano(TN), Italy.*

(Dated: November 10, 2018)

We demonstrate the violation of k_{\perp} -factorization for quark production in high energy hadronic collisions. This violation is quantified in the Color Glass Condensate framework and studied as a function of the quark mass, the quark transverse momentum, and the saturation scale Q_s , which is a measure of large parton densities. At x values where parton densities are large but leading twist shadowing effects are still small, violations of k_{\perp} -factorization can be significant – especially for lighter quarks. At very small x , where leading twist shadowing is large, we show that violations of k_{\perp} -factorization are relatively weaker.

The k_{\perp} -factorization formalism [1], devised originally for heavy quark production in hadronic collisions, systematically resums powers of $\alpha_s \ln(s/q_{\perp}^2)$ in perturbative QCD. These contributions are important at high energies when the transverse momentum q_{\perp} of the final state is much smaller than the center of mass energy \sqrt{s} . In the k_{\perp} -factorization framework, the quark production cross-section is expressed as the convolution of a hard matrix element and distribution functions from each of the two hadrons. These “unintegrated” gluon distributions depend on the longitudinal momentum fraction x and the transverse momentum \mathbf{k}_{\perp} of the gluon taking part in the hard scattering. When integrated over all transverse momenta up to some hard scale M^2 , these distributions give the more familiar gluon distribution $xG(x, M^2)$.

Even though logarithms due to gluon branchings are resummed in the framework of refs. [1], only one hard gluon from each projectile participates in the reaction. It is interesting to consider whether the k_{\perp} -factorization framework can be extended beyond the single hard scattering (leading twist) case. The simplest experiments for studying hard multiple scattering (higher twist) effects are those where one of the projectiles is dilute and the other is dense. These include a) p-p collisions in the forward/backward fragmentation region at the Relativistic Heavy Ion Collider (RHIC) and the Large Hadron Collider (LHC), where large x 's in one projectile and small x 's in the other are probed, and b) proton or Deuteron collisions off large nuclei at RHIC and LHC. Understanding the validity of k_{\perp} factorization in this multiple scattering regime is important for a quantitative understanding of final states at RHIC and LHC.

The Color Glass Condensate (CGC) [2], wherein the two projectiles are sources of classical color fields, is a powerful framework to study multiple scattering effects.

The leading twist results of refs. [1] for quark pair production are easily recovered in this formalism [3] keeping only terms that are of lowest order in the sources. k_{\perp} -factorization was studied in the forward p-p/p-A case, where one keeps the lowest order in one of the sources and all orders in the other source – this power counting is discussed further after eq. (4). In refs. [4, 5], this formalism was used to obtain the cross-section for gluon production in p-A collisions, which was found to be k_{\perp} -factorizable in [5, 6]. Quark production in p-A collisions was computed in the CGC formalism in [7, 8]. It was shown explicitly in [7] that both quark pair production and single inclusive quark cross-sections are not k_{\perp} -factorizable [12]. In this note, we quantify, for the first time, the magnitude of the violation of k_{\perp} factorization.

The generalization of the leading twist formula of refs. [1] for the inclusive quark production cross-section in p-A collisions gives [7],

$$\begin{aligned} \frac{d\sigma_Q}{d^2\mathbf{q}_{\perp} dy_q} &= \frac{\alpha_s^2 N}{8\pi^4(N^2 - 1)} \int \frac{dp^+}{p^+} \int_{\mathbf{k}_{1\perp}, \mathbf{k}_{2\perp}} \frac{1}{\mathbf{k}_{1\perp}^2 \mathbf{k}_{2\perp}^2} \\ &\times \left\{ \text{tr} \left[(\not{q} + m) T_{q\bar{q}}(\not{p} - m) T_{q\bar{q}}^* \right] \frac{C_F}{N} \phi_A^{q,q}(\mathbf{k}_{2\perp}) \right. \\ &+ \int_{\mathbf{k}_{\perp}} \text{tr} \left[(\not{q} + m) T_{q\bar{q}}(\not{p} - m) T_g^* \right] \phi_A^{q\bar{q},g}(\mathbf{k}_{2\perp}; \mathbf{k}_{\perp}) + \text{h.c.} \\ &\left. + \text{tr} \left[(\not{q} + m) T_g(\not{p} - m) T_g^* \right] \phi_A^{g,g}(\mathbf{k}_{2\perp}) \right\} \varphi_p(\mathbf{k}_{1\perp}), \quad (1) \end{aligned}$$

where the shorthand notation corresponds to the explicit expressions,

$$\begin{aligned} T_{q\bar{q}}(\mathbf{k}_{1\perp}, \mathbf{k}_{\perp}) &\equiv \\ &= \frac{\gamma^+ (\not{q} - \not{k} + m) \gamma^- (\not{q} - \not{k} - \not{k}_{\perp} + m) \gamma^+}{2p^+ [(q_{\perp} - \mathbf{k}_{\perp})^2 + m^2] + 2q^+ [(q_{\perp} - \mathbf{k}_{\perp} - \mathbf{k}_{1\perp})^2 + m^2]} \\ T_g(\mathbf{k}_{1\perp}) &\equiv \frac{\not{C}_L(p + q, \mathbf{k}_{1\perp})}{(p + q)^2}. \quad (2) \end{aligned}$$

C_L^μ is the well known Lipatov effective vertex. In eq. (1), $\mathbf{k}_{1\perp}$ and $\mathbf{k}_{2\perp}$ are respectively the transverse momenta transferred from the proton and the nucleus, and \mathbf{p}_\perp must be understood as $\mathbf{k}_{1\perp} + \mathbf{k}_{2\perp} - \mathbf{q}_\perp$. All the relevant information about the proton and the nucleus is encoded in the function φ_p and in the various ϕ_A 's respectively. These are defined as

$$\varphi_p(l_\perp) \equiv \frac{\pi^2 R_p^2 g^2}{l_\perp^2} \int_{\mathbf{x}_\perp} e^{i l_\perp \cdot \mathbf{x}_\perp} \langle \rho_1^a(0) \rho_1^a(\mathbf{x}_\perp) \rangle, \quad (3)$$

for the proton, and

$$\begin{aligned} \phi_A^{q,q}(l_\perp) &\equiv \frac{2\pi^2 R_A^2 l_\perp^2}{g^2} \int_{\mathbf{x}_\perp} e^{i l_\perp \cdot \mathbf{x}_\perp} \text{tr} \langle \tilde{U}(0) \tilde{U}^\dagger(\mathbf{x}_\perp) \rangle, \\ \phi_A^{g,g}(l_\perp) &\equiv \frac{\pi^2 R_A^2 l_\perp^2}{g^2 N} \int_{\mathbf{x}_\perp} e^{i l_\perp \cdot \mathbf{x}_\perp} \text{tr} \langle U(0) U^\dagger(\mathbf{x}_\perp) \rangle, \\ \phi_A^{q\bar{q},g}(l_\perp; \mathbf{k}_\perp) &\equiv \frac{2\pi^2 R_A^2 l_\perp^2}{g^2 N} \int_{\mathbf{x}_\perp, \mathbf{y}_\perp} e^{i(\mathbf{k}_\perp \cdot \mathbf{x}_\perp + (l_\perp - \mathbf{k}_\perp) \cdot \mathbf{y}_\perp)} \\ &\quad \times \text{tr} \langle \tilde{U}(\mathbf{x}_\perp) t^a \tilde{U}^\dagger(\mathbf{y}_\perp) t^b U_{ba}(0) \rangle \end{aligned} \quad (4)$$

for the nucleus. R_p and R_A are the radii of the proton and the nucleus respectively. U is a Wilson line in the adjoint representation, and \tilde{U} is a Wilson line in the fundamental representation. The function φ_p , expressed here in terms of the color charge density ρ_1^a in the proton, is the usual leading twist unintegrated gluon distribution of the proton [3]. The functions ϕ_A , on the other hand, include higher twist re-scattering corrections to all orders in ρ_2^a/l_\perp^2 , the ratio of the color charge density in the nucleus divided by the square of the momentum l_\perp^2 transferred from the nucleus. These correlators, and models to compute these, will be discussed further shortly. We will only mention here that the three ϕ_A 's obey, in full generality, the sum rules,

$$\begin{aligned} \int \frac{d^2 l_\perp \phi_A^{g,g}(l_\perp)}{(2\pi)^2 l_\perp^2} &= \frac{C_F}{N} \int \frac{d^2 l_\perp \phi_A^{q,q}(l_\perp)}{(2\pi)^2 l_\perp^2} = \frac{2\pi^2 R_A^2 C_F}{g^2}, \\ \int \frac{d^2 \mathbf{k}_\perp}{(2\pi)^2} \phi_A^{q\bar{q},g}(l_\perp; \mathbf{k}_\perp) &= \phi_A^{g,g}(l_\perp). \end{aligned} \quad (5)$$

Equation (1) has another important property. When integrated over p^+ , the Dirac traces that appear in this formula become independent of q^+ , or equivalently, of the rapidity of the produced quark. In a model like the McLerran-Venugopalan (MV) model [10], where the distributions φ_p and ϕ_A are independent of x , the single-quark cross-section is rigorously rapidity independent. When the distributions have an x dependence, it is a priori not legitimate to integrate the Dirac traces over p^+ because of the p^+ dependence in the x variables. However, doing so is a good approximation if the p^+ dependence of the Dirac traces is much stronger than that of the unintegrated gluon distributions. In this approximation, the integral over p^+ of the Dirac traces can then be

done in closed form. One of these is particularly simple and gives

$$\int_0^{+\infty} \frac{dp^+}{p^+} \text{tr} \left[(\not{q} + m) T_{q\bar{q}} (\not{q} - m) T_{q\bar{q}}^* \right] = 8. \quad (6)$$

Therefore, the sum rule obeyed by the distribution $\phi_A^{g,q}$ applies for this term and we can replace the factor $(C_F/N)\phi_A^{q,q}$ by $\phi_A^{g,g}$ without changing the result. Thus the only term in eq. (1) that truly breaks k_\perp -factorization is the term involving the 3-point correlator $\phi_A^{q\bar{q},g}$. For the other two terms in the cross-section, the result of the analytic integration over p^+ is rather involved and will not be quoted here.

We shall now compute the correlators in eqs. (3) and (4) in models which give good results in specific kinematic regions. As discussed more extensively in [5], studies of Gold-Gold and Deuteron-Gold collisions at RHIC suggest that the classical MV model, where the expectation values of the Wilson line operators are computed with Gaussian source functionals, is a good model for source distributions of large nuclei at moderately small x ($x \sim 10^{-2}$). In this kinematic region, where small x quantum evolution is not dominant, multiple scattering contributions can be interpreted entirely as higher twist effects. These die away rapidly with transverse momentum. When small x quantum evolution becomes significant, the Gaussian distribution of sources breaks down. The evolution of the source distributions at smaller values of x is described by a functional renormalization group (RG) equation [2] which remains to be solved. However, at very high parton densities, color charges are strongly screened allowing the application of mean field techniques analogous to the well known Random Phase Approximation. In this limit, the source functional is remarkably also a Gaussian, though (crucially) a non-local one [11]. Unlike the local MV model, which does not include non-trivial screening and recombination effects, one obtains leading twist shadowing from this Gaussian mean field model (GMF). As discussed in [5], it is conceivable that this regime might already be reached for $x \sim 10^{-3}$ in large nuclei. In the absence of a full solution of the RG equations, the MV model and the GMF model correspond to two extremes of high parton density behavior. We expect more quantitative results for single quark production to lie between these two extremes.

In Appendix A of ref. [7], we derived analytic expressions for the correlators of Wilson lines that appear in the ϕ_A 's when the distribution of color sources in the nucleus is a Gaussian, be they local or non-local. We shall use these results here. The 2-point correlators for these models in momentum space are easily computed since they reduce to a 1-dimensional integral. This follows from rotational symmetry in the transverse plane. The 3-point function $\phi_A^{q\bar{q},g}$ is more computationally intensive because it is determined by a 3-dimensional Fourier

integral. k_{\perp} -factorization requires that the 3-point and 2-point correlators are related by [7]

$$\phi_A^{q\bar{q}:g}(l_{\perp}; \mathbf{k}_{\perp}) = \frac{1}{2}(2\pi)^2 [\delta(\mathbf{k}_{\perp}) + \delta(\mathbf{k}_{\perp} - l_{\perp})] \phi_A^{g:g}(l_{\perp}). \quad (7)$$

This can be checked by substituting this relation in eq. (1). The ratio, for the MV model, between the exact 3-point function and the 2-point function $\phi_A^{g:g}$ as a function of \mathbf{k}_{\perp} at fixed l_{\perp} is displayed in figure 1. At large

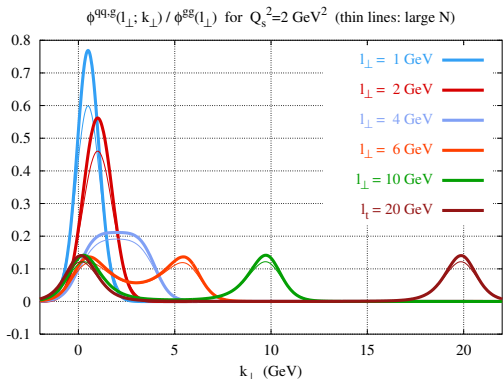


FIG. 1: The ratio $\phi_A^{q\bar{q}:g}(l_{\perp}; \mathbf{k}_{\perp})/\phi_A^{g:g}(l_{\perp})$ as a function of \mathbf{k}_{\perp} (along a line parallel to l_{\perp} in the \mathbf{k}_{\perp} plane) for various values of l_{\perp} and $Q_s^2 = 2$ GeV 2 . The thin lines represent the same ratio evaluated with the large N approximation for the 3-point correlator in the numerator.

enough l_{\perp} , this ratio indeed has two peaks centered at $\mathbf{k}_{\perp} = 0$ and $\mathbf{k}_{\perp} = l_{\perp}$ respectively. The width of these peaks is roughly of the order of the saturation momentum in the nucleus, Q_s . Eventually, when l_{\perp} decreases below a value of order Q_s , the two peaks merge into a single maximum centered at $l_{\perp}/2$. This behavior of the three point correlator suggests that k_{\perp} -factorization is a good approximation if the produced quark is characterized by some large momentum scale (m or q_{\perp}). Indeed, if this is the case, the typical $\mathbf{k}_{2\perp}$ in eq. (1) is large compared to Q_s , and eq. (7) is a good approximation of the two-peak structure of the exact 3-point function.

In the large N limit, the 3-point function in the MV and GMF models is a product of two 2-point functions. The validity of the large N computation of the 3-point function (represented by thin lines in figure 1) is reasonably good. In figure 2, we compare the quark cross-sections obtained in the full calculation with those in the large N approximation computed for $N = 3$. They are close to one another since terms neglected in the large N limit are of order $1/N^2$. We shall therefore perform all subsequent numerical calculations in the large N approximation.

We shall now discuss the violation of k_{\perp} -factorization in cross-sections. In Fig. 3, we plot the ratio of the complete result to the k_{\perp} factorized result (obtained by using

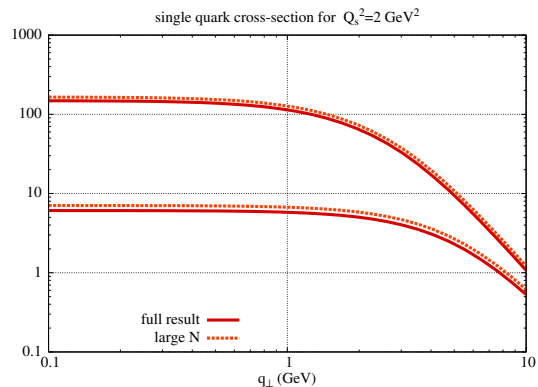


FIG. 2: Comparison of the cross sections obtained with the exact 3-point function and with the large N approximation, for $Q_s^2 = 2$ GeV 2 , $m = 1.5$ GeV and $m = 4.5$ GeV.

eq. (7) for the 3-point function) as a function of the transverse momentum in the MV model, respectively for quark masses $m = 0.15$ GeV, $m = 1.5$ GeV and $m = 4.5$ GeV. The various curves in each figure correspond to different values of Q_s . Extrapolating from saturation models of the HERA data (see [2] for a discussion), one estimates $Q_s^2 = A^{1/3}(x_0/x)^\lambda$, where $x_0 = 3 \cdot 10^{-4}$ and $\lambda \approx 0.3$. The values of Q_s^2 shown in Fig. 3 correspond to a wide range of x . The values of $Q_s^2 = 1$ GeV 2 and 4 GeV 2 correspond to the central regions at RHIC and LHC respectively. Larger values of 15 and 25 GeV 2 correspond to very forward kinematics-between 4 and 6 units of rapidity in the proton direction in future proton-Lead experiments at the LHC; large values of Q_s may also be accessed in proposed upgrades at RHIC.

From the figure 3, one can clearly deduce the following:

- (1) The breaking of k_{\perp} -factorization is quite sensitive to the quark mass. The magnitude of the breaking is systematically smaller for heavier quarks because they are less sensitive to re-scattering effects than light quarks.
- (2) The magnitude of the breaking for the heavier quarks becomes significant only at values of the saturation scale that correspond to forward rapidities. Isolating these effects from other uncertainties in these measurements is difficult but can be done in principle. One might have to look simultaneously at other final states, such as hard diffractive final states, that are also sensitive to three point functions.
- (3) The magnitude of its breaking is maximal for $q_{\perp} \sim Q_s$. One recovers k_{\perp} -factorization when the quark transverse momentum is much larger than Q_s .
- (4) If Q_s remains smaller than the quark transverse mass, the breaking of k_{\perp} -factorization enhances the cross-section because re-scatterings push a few more $Q\bar{Q}$ pairs above the pair production threshold. Conversely, if Q_s is large relative to the quark mass, the cross-section is reduced at small transverse momentum because multiple scatterings typically transfer large transverse momenta

to the quark.

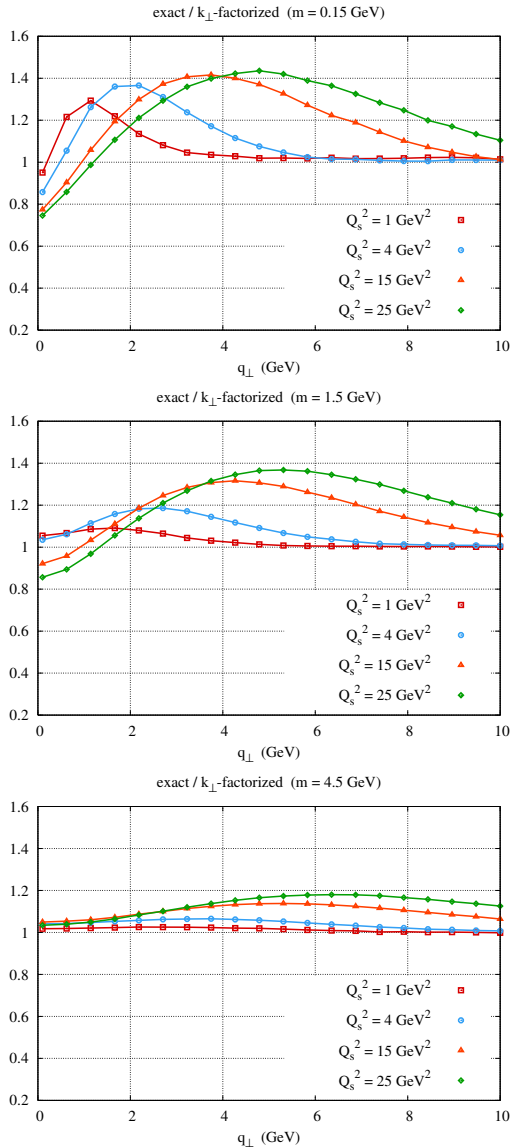


FIG. 3: Breaking of k_{\perp} -factorization in the MV model, respectively for strange, charm and bottom quark production.

As discussed previously, these conclusions in MV model are valid when parton densities are high but quantum evolution is not significant. Computing the same quantities in the GMF model provides a good idea of the direction and magnitude of the effects when small x quantum evolution becomes significant. The results in figure 4 for the production of charm quarks, display the same trends outlined previously. The magnitude of the breaking of k_{\perp} -factorization is relatively smaller in this model. Similar results were obtained in our previous study [5] of re-scattering effects in gluon production. An intuitive way to understand this result is to note that recombination/screening effects lead to a depletion in the number

of gluons available to re-scatter. For comparison, we also

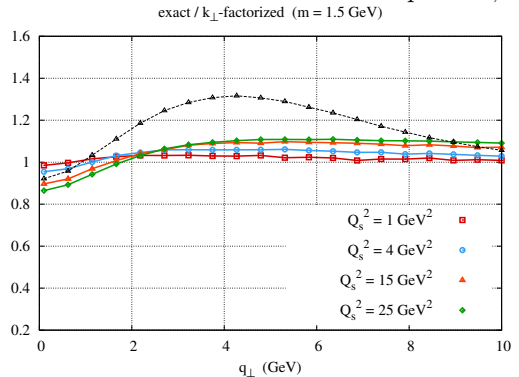


FIG. 4: Breaking of k_{\perp} -factorization for charm quarks in the non-local Gaussian effective model of [11]. The dashed line shows the result (for $Q_s^2 = 15 \text{ GeV}^2$) in the MV model for comparison.

plot the result for charm quarks at $Q_s^2 = 15 \text{ GeV}^2$ in the MV model. We expect results of detailed RG computations to lie within the band outlined in Fig. 4.

RV's research was supported in part by DOE Contract No. DE-AC02-98CH10886 and the Alexander von Humboldt foundation. He thanks the theory groups at Saclay, Univ. of Bielefeld, the Univ. of Hamburg/DESY and ECT* for their kind hospitality. HF's work is supported by the Grants-in-Aid for Scientific Research (16740132).

-
- [1] S. Catani, M. Ciafaloni, F. Hautmann, Nucl. Phys. **B 366**, 135 (1991); J.C. Collins, R.K. Ellis, Nucl. Phys. **B 360**, 3 (1991).
 - [2] E. Iancu, R. Venugopalan, hep-ph/0303204; E. Iancu, A. Leonidov, L.D. McLerran, hep-ph/0202270; A.H. Mueller, hep-ph/9911289.
 - [3] F. Gelis, R. Venugopalan, Phys. Rev. **D 69**, 014019 (2004).
 - [4] Yu.V. Kovchegov, A.H. Mueller, Nucl. Phys. **B 529**, 451 (1998); A. Dumitru, L.D. McLerran, Nucl. Phys. **A 700**, 492 (2002).
 - [5] J.P. Blaizot, F. Gelis, R. Venugopalan, Nucl. Phys. **A 743**, 13 (2004).
 - [6] Yu.V. Kovchegov, K. Tuchin, Phys. Rev. **D 65**, 074026 (2002); D. Kharzeev, Yu. Kovchegov, K. Tuchin, Phys. Rev. **D 68**, 094013 (2003).
 - [7] J.P. Blaizot, F. Gelis, R. Venugopalan, Nucl. Phys. **A 743**, 57 (2004).
 - [8] K. Tuchin, Phys. Lett. **B 593**, 66 (2004).
 - [9] N. Nikolaev, W. Schafer, B. Zakharov, hep-ph/0502018.
 - [10] L. McLerran, R. Venugopalan, Phys. Rev. **D 49**, 2233, 3352 (1994); *ibid* **50**, 2225 (1994).
 - [11] E. Iancu, K. Itakura, L.D. McLerran, Nucl. Phys. **A 724**, 181 (2003).
 - [12] The violation of k_{\perp} -factorization has been studied in a different framework. See ref. [9] and references therein.